Soft Matter

# Photoinduced repetitive separation of the supramolecular assembly composed of amphiphilic diarylethene mixture



| | |
|---|---|
| Journal: | *Soft Matter* |
| Manuscript ID | SM-ART-06-2019-001301.R1 |
| Article Type: | Paper |
| Date Submitted by the Author: | 30-Aug-2019 |
| Complete List of Authors: | Sakakibara, Seiya; Kyoto University, Department of Synthetic Chemistry and Biological Chemistry, Graduate School of Engineering<br>Yotsuji, Hajime; Kyoto University, Department of Synthetic Chemistry and Biological Chemistry, Graduate School of Engineering<br>Higashiguchi, Kenji; Kyoto University, Department of Synthetic Chemistry and Biological Chemistry, Graduate School of Engineering<br>Matsuda, Kenji; Kyoto University, Department of Synthetic Chemistry and Biological Chemistry, Graduate School of Engineering |
| | |

ARTICLE

# Photoinduced repetitive separation of the supramolecular assembly composed of amphiphilic diarylethene mixture†

Received 00th January 20xx,
Accepted 00th January 20xx

DOI: 10.1039/x0xx00000x

Seiya Sakakibara, Hajime Yotsuji, Kenji Higashiguchi* and Kenji Matsuda*

Supramolecular assembly composed of two-component mixture of amphiphilic diarylethenes, which have octyloxycarbonyl and *N*-octylcarbamoyl groups, showed unique macroscopic transformation upon irradiation with UV light and subsequent standing in the dark. Unlike the pure compounds, the assembly was repetitively separated into a blue sphere and a red-purple sparse structure. Both the blue sphere and sparse structure turned into colorless sphere upon irradiation with visible light and the divided colorless spheres showed the same response to the UV and visible lights. Phase diagrams based on the change in absorption spectra upon temperature change suggested that the transformation originates from LCST transition. In the 0.5:0.5 mixture, in contrast to the pure compounds, the transition temperature sharply changed around 50% of the fraction of the closed-ring isomer. TEM image showed that the 0.5:0.5 mixture with high photoisomerization yield formed a few ten nanometer-sized network. Judging from the phase diagram and TEM images, the separation is understood as the local phase transition of the regions of high fraction of the closed-ring isomer.

## 1. Introduction

Amphiphilic molecules aggregate with each other and form supramolecular architecture in aqueous media due to hydrophobic interaction.[1-4] Morphology of the architecture is determined by the geometrical shape and volume ratio of hydrophilic and hydrophobic moieties.[5,6] Although the complete control of the architecture remains difficult even by means of current supramolecular chemistry, design and construction of the supramolecular architecture composed of functional aromatic compounds have been reported actively.[7-12]

One of the advantages of soft assembly of amphiphilic molecules is the flexibility of the structure, which is essential for constructing networked chemical systems based on dynamic self-assembly. The supramolecular architecture assembled by hydrophobic interaction changes its structure depending on the environment. The structural changes have been reported by the change of pH,[13,14] addition of salt,[15-18] and sonication.[19-23] Meanwhile, when the external stimulus alters the structure of consisting molecule by chemical reaction, the supramolecular architecture is also altered.[24-28]

In the supramolecular systems chemistry, not only single-component assembly, but also multi-component assembly is important.[29,30] The multi-component assembly has been widely studied, for example, from the viewpoint of assembling process,[31,32] control of liquid crystals,[33,34] and energy and electron transfer.[35,36] Amphiphilic multi-component assemblies have also been reported and considerable attention has been paid.[37-41] Würthner and co-workers reported that the co-self-assembly of different shapes of perylene bisimide amphiphiles provides unique structure and unique photophysical property.[37,38]

Oligo(ethylene glycol) chain is occasionally employed to bestow hydrophilicity to organic compound and the hydrophilicity often changes upon temperature change, which is known as lower critical solution temperature (LCST).[41-53] The oligo(ethylene glycol) chain is hydrogen-bonded with water in the low-temperature phase. In contrast, in the high-temperature phase, phase separation between the chain and water occurs and the solution turns turbid. Therefore, when the structure of oligo(ethylene glycol) derivative comprising supramolecular assembly is altered by the external stimulus, the LCST temperature is also altered. When the environmental temperature is located between the LCSTs before and after the stimulus, LCST transition is triggered by the stimulus.[54-56]

Recently, we have reported photoinduced morphological transformation using LCST behavior of amphiphilic diarylethenes.[57-62] The diarylethenes having alkyl chain with ester- (**1**) and amide- (**2**) linkage as hydrophobic group and tri(ethylene glycol) chains as hydrophilic group exhibited different supramolecular architecture.[58] The photoinduced change is found to be related to LCST transition, i.e., the open-ring isomer that exists in the dehydrated high-temperature phase turned into the closed-ring isomer in the hydrated low-temperature phase. Although diarylethenes **1** and **2** had similar molecular structures, the nanostructures of supramolecular architecture were different, i.e., the ester-linked closed-ring isomer **1b** and the amide-linked one **2b** formed nanofiber and nanosheet, respectively. Photoinduced macroscopic morphological transformation was also different. While the aggregate of ester-linked diarylethene **1** showed division easily

*Department of Synthetic Chemistry and Biological Chemistry, Graduate School of Engineering, Kyoto University, Katsura, Nishikyo-ku, Kyoto 615-8510, Japan.*
†Electronic Supplementary Information (ESI) available: Movies and additional figures. See DOI: 10.1039/x0xx00000x

upon irradiation with UV light, the aggregate of amide-linked diarylethene **2** swelled but did not show division upon irradiation with UV light. The strong hydrogen bond network was found to suppress photoinduced morphological change in micrometer-sized structure.

In this paper, we report unique photoinduced morphological transformation and nanostructural change for the mixture of diarylethenes **1** and **2**. Unlike the pure compounds, upon irradiation with UV light, the 0.5:0.5 mixture showed repetitive separation of the supramolecular assembly into a blue sphere and a red-purple sparse structure. Both the blue sphere and sparse structure turned into colorless sphere upon irradiation with visible light and the divided colorless spheres showed the same response to the UV and visible lights. Phase diagram and TEM images suggest that the separation originates from the local phase transition of the regions of high fraction of the closed-ring isomer.

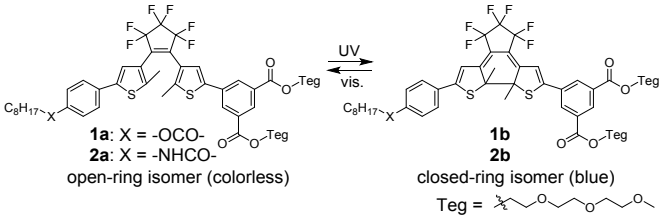


**Fig. 1** Photochromic reaction of amphiphilic diarylethenes **1** and **2**.

## 2. Experimental section

### 2.1 Preparation of materials

Syntheses of amphiphilic diarylethenes **1** and **2** were previously reported.[58] Other commercially available compounds and solvents were used as received.

Suspensions containing **1** and **2** were prepared in the similar manner as described in the previous literature.[58] A representative method was as follows: two solutions of each diarylethene in acetonitrile (10 mM) were mixed in the appropriate volume ratio, and consequently the solution (50 μL) was injected into pure water (1 mL) at room temperature, then a colorless suspension was obtained (0.50 mM). The photoisomerization yield to the closed-ring isomer was controlled upon irradiation with UV and visible lights. The suspension was analyzed by HPLC for determination of the composition ratio and the photoisomerization yield as shown in Figs. S1 and S2. The analyses were carried out on a HITACHI LC System LaChrom. Analytical (Kanto Chemical, Mightysil RP-18(H) GP250-4.6 (5 μm)) column and $CH_3CN$ (1 mL $min^{-1}$) was used for the separation. Detection wavelength was set at 311 nm, where molar absorption coefficient of each isomer was almost the same (open-ring isomer: $\varepsilon_{\mathbf{1a},311} = 3.87 \times 10^4$ and $\varepsilon_{\mathbf{2a},311} = 3.85 \times 10^4$ $M^{-1}$ $cm^{-1}$; closed-ring isomer: $\varepsilon_{\mathbf{1b},311} = 2.74 \times 10^4$ and $\varepsilon_{\mathbf{2b},311} = 2.77 \times 10^4$ $M^{-1}$ $cm^{-1}$).

### 2.2 Measurement of photoinduced morphological transformation

Experimental procedures for photoisomerization of the suspension, observation of photoinduced transformation under optical microscope, and TEM observation are the same as our previous literature.[58]

The measurement of temperature-dependent spectral change was similar to our previous literature.[58] The UV-vis spectra of diarylethenes in aqueous suspensions were recorded with a JASCO V-670 spectrometer equipped with ETCS-761 Peltier temperature controller for cuvette. The representative temperature ranges were 0-50 °C at 1 °C intervals and 0-20 °C at 0.5 °C intervals for the suspensions having high and low photoisomerization yield, respectively. The cooling and heating rate was 1.0 °C $min^{-1}$. The suspension was kept at the set temperature for 5 min with stirring at 600 rpm before measurement.

The transition temperature was determined by the change of absorption maximum wavelength. The shift of absorption maximum wavelength ($\lambda_{max}$) was plotted in the cooling and heating process and fitted by Boltzmann sigmoidal function (eq. 1),

$$\lambda_{max}(T) = \frac{\lambda_{max,L} - \lambda_{max,H}}{1 + \exp[(T - T_0)/a]} + \lambda_{max,H} \quad (1)$$

where $\lambda_{max,L}$, $\lambda_{max,H}$, $T_0$, and $a$ are absorption maximum wavelength at low and high end temperature, the point of inflexion of the sigmoidal curve, and fitting constant, respectively. In the previous literature,[58] the transition temperature had been determined by onset of cooling period, which was calculated using a tangential line at $T_0$. However, average temperature in the cooling and heating processes was employed in this study because the hysteresis curve of the 0.5:0.5 mixture was larger than pure **1** and **2**. Therefore, the phase boundaries of pure **1** and **2** were redetermined by the same method for comparison (Fig. 6a, dotted and dashed lines). When the shift was scarcely detected due to the precipitation, the integrated O.D. change between 250 and 800 nm was employed, which is shown in Fig. S14.

## 3. Results and discussion

### 3.1 Photo- and thermoresponsive behavior of supramolecular assembly consisting of 1 and 2

The mixed aggregates were prepared by addition of pure water into acetonitrile solution of ester- and amide-linked diarylethenes **1** and **2**, whose content was controlled using volume ratio of each solution having the same concentration. The acetonitrile was not removed from the suspension. The composition ratio **1**:**2** in the suspension was naturally the same as the volume ratio, which was confirmed by HPLC.

In the previous work, we reported the photoinduced morphological change of the supramolecular architecture composed of pure diarylethene **1** or **2**.[58] The open- and the closed-ring isomers showed LCST transition at lower and higher temperature than room temperature, respectively. Therefore, the supramolecular architecture showed phase transition from the high-temperature dehydrated phase composed of the open-ring isomer to the low-temperature-hydrated phase composed of the

 

closed-ring isomer along with the photoisomerization from the open- to the closed-ring isomer. This phenomenon is regarded as photoinduced LCST transition. The open-ring isomer formed bicontinuous coacervate-type supramolecular architecture, corresponding to the dehydrated phase of LCST. In contrast, the morphology of the hydrated phase of LCST composed of the closed-ring isomer was fiber or sheet.

The mixed aggregate showed phase transition by light irradiation and temperature change as observed for pure diarylethenes **1** and **2**. Figs. 2a and b show the change in absorption spectra of the aqueous suspension containing **1**:**2** = 0.49:0.51 and the shift of its maximum wavelengths, respectively. In the initial state, the scattering due to the aggregates of the open-ring isomer raised the baseline up to 800 nm. Upon irradiation with UV (365 nm) light, the absorbance around 640 nm increased initially. Subsequent irradiation with UV light gave rise to a new band around 570 nm and the band around 640 nm remained as a shoulder. This blue shift suggests the formation of H-aggregates, which is a very similar behavior to pure diarylethenes **1** and **2**. The H-aggregate appeared by cooling from 60 to 0 °C and disappeared by subsequent heating of the colored suspension as shown in Figs. 2c and d, which is also the same as pure **1** and **2**. When the sample with different molar ratio of **1**:**2** was used, very similar spectral change was observed (Figs. S9-S12).

We noticed that the size of hysteresis loop of heating and cooling processes is different between the mixture and the pure compounds when the hysteresis loop is examined under various rates of temperature control. The mixture having 54% of photoisomerization yield had large hysteresis loop (16 °C) at the rate of 1 °C $min^{-1}$, while pure **1** and **2** showed small hysteresis (6-10 °C) as shown in Fig. S3. Therefore, the mixture is considered to undergo slow reorientation compared to pure **1** and **2**. In addition, the mixture showed slow formation of H-aggregate under continuous irradiation with UV light compared to pure **1** and **2**, which also supported the slow reorientation (Fig. S4). The required time for reorientation was determined by time course of spectral shift in the dark as ca. 100 min as shown Fig. S4d.

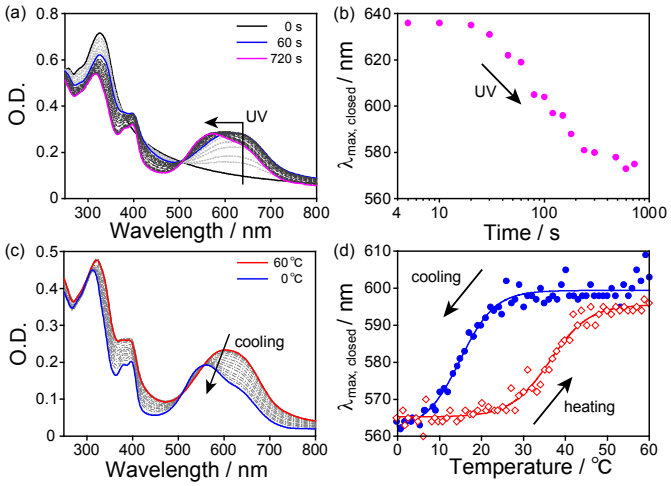


**Fig. 2** (a) The spectral change during continuous irradiation with UV (365 nm) light for the suspension containing **1**:**2** = 0.49:0.51: initial, black line; 60 s, blue line; 720 s, purple line. Pale gray dotted lines and dark gray dashed lines indicate spectral change from 0 to 60 and from 60 to 720 s, respectively. (b) The change in absorption maxima around 580 nm. (c) The spectral change of the suspension containing **1**:**2** = 0.47:0.53 at 54% photoisomerization yield upon cooling from 60 (red solid line) to 0 °C (blue solid line). (d) The change in absorption maxima around 580 nm upon cooling (blue filled circles) and heating (red open diamonds).

### 3.2 Photoinduced morphological transformation

The photoinduced morphological change was observed for the micrometer-sized assembly composed of **1**:**2** = 0.5:0.5 mixture under an optical microscope. Although the absorption spectral change was similar between the mixture and the pure compounds, the macroscopic morphological change was remarkably different. The repetitive irradiation with UV light led the repetitive formation of sparse structure from the same microsphere as shown in Movie S1 and Fig. 3. When irradiation of UV light was carried out from top of the microsphere under optical microscope for 10 s at 5 °C, the upper side of the sphere was mainly colored due to the preferential photoisomerization (Fig. 3a). Subsequently, semitransparent sparse structure was generated progressively from the colored microsphere by standing in the dark for 3.8 min (Fig. 3b). The remained blue sphere and separated transparent purple structure are considered to be random- and H-aggregated states, respectively. The sparse structure moved by Brownian motion after additional standing in the dark for 5 min (Fig. 3c) and finally separated from the original microsphere. Figs. 3d-f shows the second formation from the same microsphere. The schematic illustrations of separation of sparse structures are also shown in insets. Figs. 3g and h show the result of repetitive separation for five times and subsequent shrinking into microspheres. The separated sparse structures kept their structure for 3 h without deformation or dispersion under weak observation light.

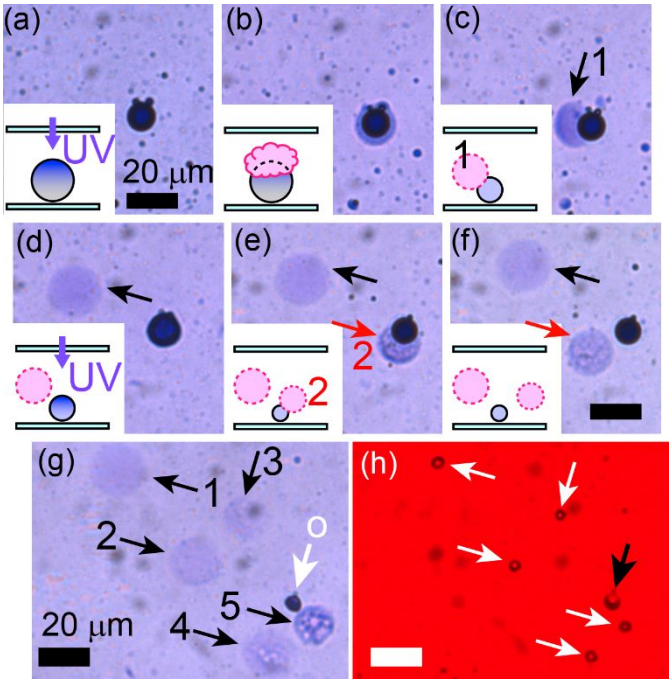


**Fig. 3** Separation of the supramolecular assembly composed of **1**:**2** = 0.5:0.5 by repetitive irradiation with UV light from top of the precipitated

microsphere at 5 °C. (a) After irradiation with UV light for 10 s, (b) generation of sparse structure at the top of microsphere after standing in the dark for 3.8 min, (c) moving of the sparse structure by Brownian motion after additional standing in the dark for 5.0 min, (d) separation of first sparse structure and second irradiation with UV light, (e) second moving, and (f) second separation. Schematic illustrations show mechanism of the division from side of the cell. (g) After repetitive operation for 5 times and (h) change to sphere upon irradiation with visible light. The red hue in (h) is due to the filters used to remove irradiated green light.

The morphological change was observed in the different conditions of temperature and irradiation time. Fig. 4 shows the behavior of photoinduced LCST transition by changing the temperature and irradiation time under the optical microscope. In the region of high temperature and short irradiation time, the separation of sphere was not observed because of insufficient photoisomerization yield for the LCST. At the temperature higher than 14 °C, the separation of sphere was never observed. Meanwhile, in the region of low temperature and long irradiation time, the separation also did not occur because the LCST completely took place and no sphere remained. It is suggested that there is an optimal condition for the separation of sparse structure from the sphere. At 5 °C, the observation of separation was easily observed, so that the following experiment was performed at 5 °C.

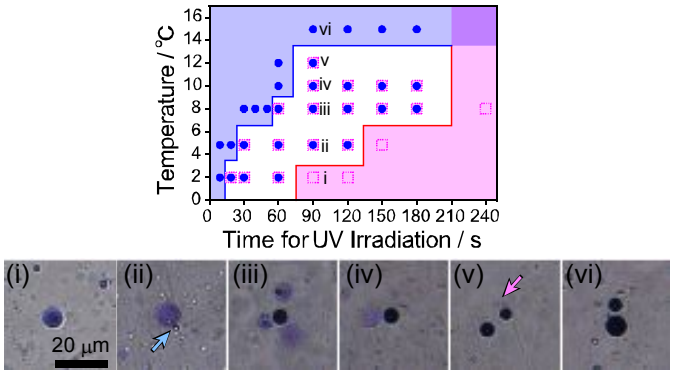


**Fig. 4** The behavior of phase transition related to irradiation time and temperature under the optical microscope. Dehydrated blue sphere (blue filled circle) and hydrated red-purple sparse structure (purple dotted square) were observed in the blue and red region, respectively. The white region was the optimal condition for the separation of sparse structure from the sphere (blue circle overlaid on purple square). (i-vi) Optical images of the separation observed under various temperature. The time for exposure of UV (365 nm) light was the same (90 s). Sky blue and pink arrows indicate small remained sphere and separated sparse structure, respectively.

Weak UV light compared with Figs. 3 and 5 was employed. The divided sparse structure returned to sphere by visible light and again showed separation upon irradiation with UV light as shown in Movie S2 and Fig. 5. Figs. 5a-c shows the separation of sparse structure at 5 °C as described above. In Fig. 5d, both the sparse structure and colored microsphere returned to colorless microspheres upon irradiation of visible light. Both spheres showed the morphological change again and divided into four as shown in Figs. 5e-g.

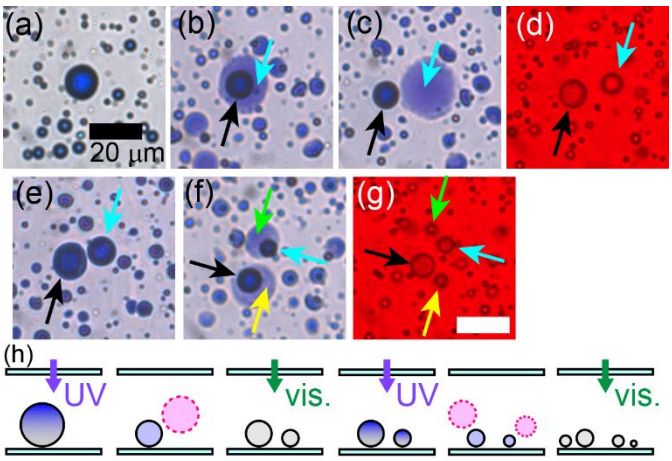


**Fig. 5** Division of microspheres composed of **1**:**2** = 0.5:0.5 by repetitive irradiation with UV and visible lights from top of the precipitated microsphere at 5 °C. (a) At the initial state, (b) generation of sparse structure upon irradiation with UV light for 10 s and the standing for 9 min, (c) separation by keeping for 6 min, (d) shrinking upon irradiation with visible light for 20 s, (e) second irradiation with UV light, (f) the second separation, and (g) the second shrinking. The corresponding supramolecular assemblies are labelled by the colored arrows. The red hues in (d) and (g) are due to the filters used to remove irradiated green light.

Judging from the fact that the divided two spheres showed the generation of the sparse structure simultaneously, it is considered that the composition ratios of the original and separated spheres were almost the same. If the composition ratios were different between the two spheres, the behavior of the photoinduced generation of sparse structure should be different.

Fig. S18 shows the result of the same experiment using pure **1** or **2** or the mixture of **1**:**2** = 0.80:0.20. In all cases, generation of the sparse structure was not observed. This result suggests that the generation of the sparse structure was the unique phenomenon for the mixture composed of **1**:**2** = 0.5:0.5.Because the mixture showed unique behavior, the miscibility between **1** and **2** was investigated by phase transition behavior. Homogeneity can be assessed by the fact that homogeneous and heterogeneous mixtures should have one- and two-step phase-transition curves, respectively. An aqueous suspension, whose composition ratio was **1**:**2** = 0.47:0.53 and the photoisomerization yield to the closed-ring isomer was 54%, was prepared. The shift of absorption maximum wavelength, which was caused by H-aggregate structure of the closed-ring isomers, appeared as one-step transition upon temperature change (Fig. 2d). Homogeneity was confirmed also by the experiment on the suspensions prepared by two distinct methods from diarylethenes **1** and **2** with different photoisomerization yields (66 and 13% for **1** and **2**, respectively): method (i), the acetonitrile solutions of **1** and **2** were mixed and then injected into water; method (ii), the acetonitrile solutions of **1** and **2** were injected into water independently and then mixed. The sample prepared by method (i) showed one-step phase transition (Fig. S15a), while the sample prepared by method (ii) showed two-step phase transition (Fig. S15d). Because no aggregate is formed in the acetonitrile solution, it is considered that the aggregate was formed immediately after the acetonitrile solution

was injected into water. This result confirms that the supramolecular aggregate is estimated as homogeneous mixture.

### 3.3 Phase diagram

Phase diagrams of the LCST transition were plotted based on the change in absorption spectra upon temperature change. Fig. 6a shows the diagram of **1**:**2** = 0.5:0.5 mixture against various photoisomerization yield. In the diagram, red and blue regions correspond to the hydrated and dehydrated phases, respectively. The boundary appeared as sigmoidal curve, i.e., the LCST transition temperature of the supramolecular assembly sharply changed against photoisomerization yield at around 50%. In contrast, the boundary line of pure **1** and **2** linearly changed along with photoisomerization as reported previously (Fig. 6a, gray dotted and dashed lines). It means that the open- and closed-ring isomers could be miscible with each other in pure **1** and **2**. The phase diagram of the open-ring isomer against various composition ratio **1**:**2** shows the linear dependence of transition temperature on composition ratio, suggesting that the open-ring isomers **1a** and **2a** were also miscible (Fig. 6b). In the mixture of **1**:**2** = 0.5:0.5, it is suggested that the LCST transition occurs abruptly during photoisomerization reaction. This sigmoidal phase diagram should be related to the unique photoinduced morphological change described in the previous section.

The two-dimensional phase diagram against both the composition ratio **1**:**2** and the photoisomerization yield from the open- to the closed-ring isomer was plotted as a heat map (Fig. S13) based on the transition temperature with various composition ratio and photoisomerization yield (Figs. S5-S12 and Tables S1-S4). The diagram at 5 °C is shown in Fig. 6c. TEM investigations of nanostructures described below were carried out at 5 °C following yellow and green arrows in this figure.

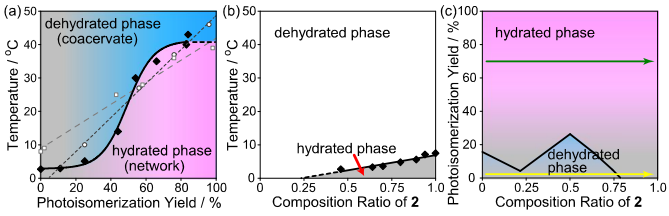


**Fig. 6** Phase diagrams of the LCST transition in aqueous suspension of (a) the mixture of **1**:**2** = 0.5:0.5 against photoisomerization yield, (b) the colorless open-ring isomer against composition ratio. (c) Two-dimensional phase diagram at 5 °C against both composition ratio and photoisomerization yield. In (a), filled diamonds with solid line, open circles with dotted line, and open squares with dashed line indicate the boundary obtained from the assembly composed of **1**:**2** = 0.5:0.5, 1:0, and 0:1, respectively. The change in absorption spectrum and absorption maximum for panel (a) are shown in Figs. S5 and S6, and Table S1. The data for panel (b) are shown in Figs. S7 and S8, and Table S2. The yellow and green arrows in panel (c) correspond to TEM images shown in Figs. 7a-e and 7f-j, respectively.

### 3.4 TEM observation

TEM observation was carried out in order to investigate supramolecular nanostructure corresponding to respective regions of the phase diagram (Fig. 7). Nanostructures of pure **1** and **2** has been reported in the previous literature.[58] At 5 °C, the open-ring isomers **1a** and **2a** formed coacervate and bilayer-nanoflower (Figs. 7a and e) and the closed-ring isomers **1b** and **2b** formed nanofiber and bilayer (Figs. 7f and j), respectively. Because the nanostructures are different between pure **1** and **2**, and also different between the open- and the closed-ring isomer, nanostructure of mixed aggregate should depend on the composition ratio **1**:**2** and the photoisomerization yield from the open- to the closed-ring isomer.

Figs. 7a-e show the change in nanostructure composed of the open-ring isomer depending on the composition ratio of **1a** and **2a** (yellow arrow in Fig 6c). When the composition ratio was **1a**:**2a** = 0.75:0.25 and 0.5:0.5, coacervate structures were observed. On the other hand, foliated sheets with a few hundred nanometer-length, which was similar to pure **2**, were formed from **1a**:**2a** = 0.25:0.75 mixture. The discontinuous change in nanostructures corresponds to the phase boundary around 0.25:0.75 at 5 °C.

The supramolecular architectures prepared from various composition ratio **1**:**2** with high photoisomerization yield at 5 °C were observed by TEM (Figs. 7f-j). In this condition, the aggregate is in the hydrated state (green arrow in Fig. 6c). The photoisomerization yield was controlled at ca. 60-80% by irradiation with UV (254 nm) light. When the fraction of one component was large, the structures were similar to the pure ones, i.e., the entangled nanofibers and multilayered vesicle were observed in the cases of **1**:**2** = 0.75:0.25 and 0.25:0.75, respectively (Figs. 7g and i). In the case of **1**:**2** = 0.5:0.5, network structure was observed as shown in Fig. 7h. Therefore, the **1**:**2** = 0.5:0.5 mixture showed nanostructural change between coacervate and network upon irradiation with UV and visible lights (Figs. 7c and h). The variation in nanostructure under various condition are also shown in Figs. S23-S25.

For the supramolecular assembly composed of **1**:**2** = 0.5:0.5, TEM observation was carried out after irradiation with UV light on TEM grid (Fig. 8). The generation of network structure from coacervate state was observed. Fig. 8 is the "snapshot" during the photoinduced phase transition. Because the photoirradiation was carried out on the TEM grid, monitoring of the intermediate state of photoinduced transformation was possible using TEM. The generation of the network structure and the separation from the original coacervate is considered to be the key of the generation of the sparse structure from the sphere.

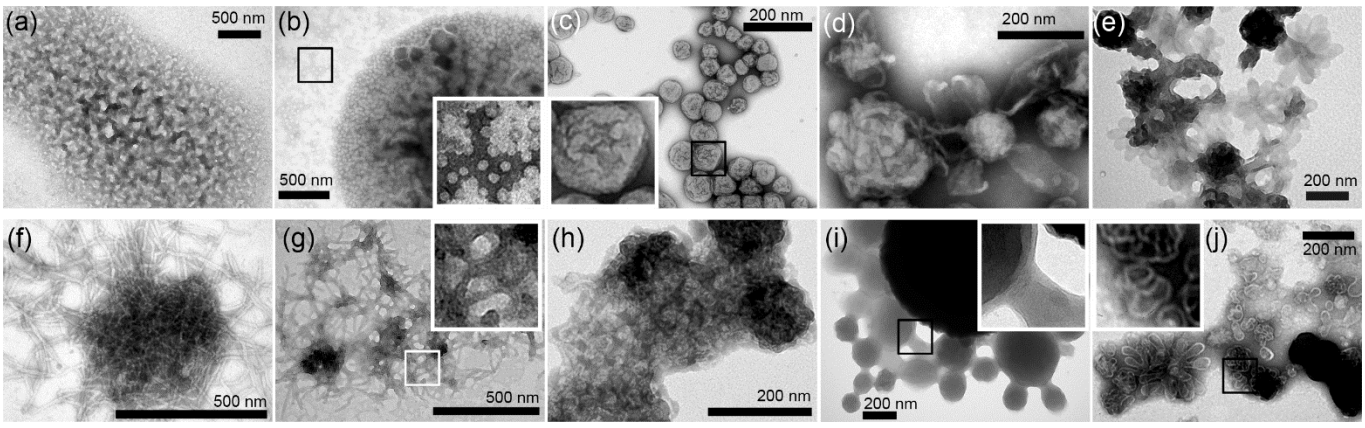


**Fig. 7** TEM images of the supramolecular architectures for various composition ratio of **1** and **2**. (a-e) Before irradiation with UV light at 5 °C corresponding to yellow arrow shown in Fig. 6c: (a) bicontinuous coacervate (**1a**:**2a** = 1:0), (b) coacervate with isolated nanospheres (0.75:0.25), (c) coacervate (0.5:0.5), (d) folded vesicles (0.25:0.75), where deformed sheets foliated with each other to form a tightly folded spherical aggregate (Fig. S24), (e) bunched vesicles (0:1). (f-j) After irradiation with UV (254 nm, photoisomerization yield ~ 70%) light at 5 °C corresponding to green arrow shown in Fig. 6c: (f) short nanofiber (**1**:**2** = 1:0), (g) tangled fiber (0.75:0.25), (h) tangled structure (0.5:0.5), (i) clustered vesicles (0.25:0.75), (j) bunched vesicles (0:1).

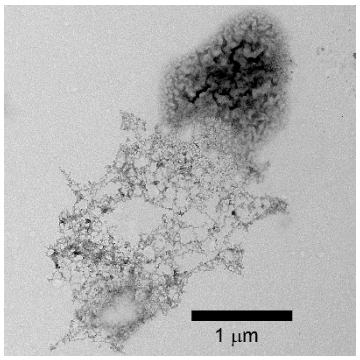


**Fig. 8** The generation of network structure from coacervate state upon irradiation with UV light for the supramolecular assembly composed of **1**:**2** = 0.5:0.5 mixture observed by TEM. The regions of coacervate and network corresponded to before and after photoisomerization to the closed-ring isomer, respectively. The irradiation was carried out under the optical microscope on TEM grid for 10 s.

### 3.5 Origin of unique photoinduced separation found for the mixture

The unique behavior of the photoinduced separation found for the mixture of **1**:**2** = 0.5:0.5 is discussed based on the result of phase diagram and TEM observation. In the phase diagram of the mixture, sigmoidal curve was observed, suggesting that the change occurs abruptly during photoisomerization reaction. Meanwhile, the phase diagram of pure **1** and **2** showed linear dependence on the photoisomerization yield. Considering that the LCST phenomenon occurs by a separation of the hydration water from the oligo(ethylene glycol) chain, the LCST temperature should have been regulated by the environment of the oligo(ethylene glycol) chain. When the molecular packing is tight and the ratio of the closed-ring isomer gets high enough to surround the remaining open-ring isomer, LCST of the open-ring isomer should be influenced by the surrounding closed-ring isomer and should show the abrupt change upon photoisomerization. In the case of pure **1** and **2**, for which no abrupt change was observed, the open- and the closed-ring isomers are considered to behave independently.

TEM images revealed that the closed-ring isomer takes network structure when the component ratio is **1**:**2** = 0.5:0.5. In other component ratios between **1** and **2**, formation of the network structure was not observed. When the network structure is formed during photoisomerization, the packing of the molecule gets tight, so that the generated surrounding closed-ring isomer can influence the LCST behavior of the remaining open-ring isomer. This network structure is considered to be the origin of the sigmoidal phase diagram observed for the mixture of **1**:**2** = 0.5:0.5.

Because the photoirradiation was performed from the top of the sample, there was a gradient of photoisomerization yield in the vertical direction. When the phase diagram is sigmoidal, the gradient gets more contrasted or bipolarized. Therefore, the upper part and lower part turned into the different phase of LCST, so that the separation can occur during photoisomerization. When low intensity of light was irradiated for long time, the separation did not occur probably due to the diffusion of the photogenerated closed-ring isomer (Fig. S20). The separation is understood as the local phase transition of the regions of high fraction of the closed-ring isomer, which originates from the sigmoidal phase diagram caused by the formation of the network structure in the mixture of **1**:**2** = 0.5:0.5.

## 4. Conclusions

In conclusion, we have observed photoinduced separation of the supramolecular assembly composed of two amphiphilic diarylethenes having an ester- (**1**) and amide- (**2**) linkage under optical microscope. The supramolecular assembly showed repetitive generation of sparse structures from the microsphere upon irradiation with UV light and standing in the dark. Both the sphere and sparse structure turned into colorless sphere upon irradiation with visible light and the divided colorless spheres showed the same response to the UV and visible lights. Judging from the phase diagram and TEM images, the separation is understood as the local phase transition of the regions of high fraction of the closed-ring isomer. This unique photoinduced transformation will widen the possibility of phototransformable smart soft material.

## Conflicts of interest

There are no conflicts to declare.

## Acknowledgements

This work was supported by a Grant-in-Aid for Scientific Research on Innovative Areas "Photosynergetics" and "Molecular Engine" (JSPS KAKENHI Grant Numbers JP26107008, JP19H05391), a Grant-in-Aid for Scientific Research (C) (JSPS KAKENHI Grant Number JP19K05400). This work was also partially supported by PRESTO, JST (Grant number JPMJPR12K7). This work was performed under the Research Program of "Dynamic Alliance for Open Innovation Bridging Human, Environment and Materials" in "Network Joint Research Center for Materials and Devices" (Number 20162025).

## References

1 S. I. Stupp and L. C. Palmer, *Chem. Mater.*, 2014, **26**, 507-518.
2 T. Shimizu, M. Masuda and H. Minamikata, *Chem. Rev.*, 2005, **105**, 1401-1443.
3 N. T. Southall, K. A. Dill and A. D. J. Haymet, *J. Phys. Chem. B*, 2002, **106**, 521-533.
4 T. Rehm and C. Schmuck, *Chem. Commun.*, 2008, 801-813.
5 B. N. S. Thota, L. H. Urner and R. Haag, *Chem. Rev.*, 2016, **116**, 2079-2102.
6 T. Kunitake, Y. Okahata, M. Shimomura, S. Yasunami and K. Takarabe, *J. Am. Chem. Soc.* 1981, **103**, 5401-5413.
7 T. Aida, E. W. Meijer and S. I. Stupp, *Science*, 2012, **335**, 813-817.
8 C. Wang, Z. Wang and X. Zhang, *Acc. Chem. Res.*, 2012, **45**, 608-618.
9 J. H. K. Ky Hirschberg, L. Brunsveld, A. Ramzi, J. A. J. M. Vekemans, R. P. Sijbesma and E. W. Meijer, *Nature*, 2000, **407**, 167-170.
10 J. P. Hill, W. Jin, A. Kosaka, T. Fukushima, H. Ichihara, T. Shimomura, K. Ito, T. Hashizume, N. Ishii and T. Aida, *Science*, 2004, **304**, 1481-1483.
11 P. Rajdev, M. R. Molla and S. Ghosh, *Langmuir*, 2014, **30**, 1969-1976.
12 N. M. Matsumoto, R. P. M. Lafleur, X. Lou, K.-C. Shih, S. P. W. Wijnands, C. Guibert, J. W. A. M. van Rosendaal, I. K. Voets, A. R. A. Palmans, Y. Lin and E. W. Meijer, *J. Am. Chem. Soc.*, 2018, **140**, 13308-13316.
13 S. Goskulwad, D. D. La, M. A. Kobaisi, S. V. Bhosale, V. Bansal, A. Vinu, K. Ariga and S. V. Bhosale, *Sci. Rep.*, 2018, **8**, 11220.
14 Q. Duan, Y. Cao, Y. Li, X. Hu, T. Xiao, C. Lin, Y. Pan and L. Wang, *J. Am. Chem. Soc.*, 2013, **135**, 10542-10549.
15 H.-J. Kim, S.-K. Kang, Y.-K. Lee, C. Seok, J.-K. Lee, W.-C. Zin and M. Lee, *Angew. Chem. Int. Ed.*, 2010, **49**, 8471-8475.
16 J. E. Betancourt and J. M. Rivera, *Langmuir*, 2015, **31**, 2095-2103.
17 Y. Ping, D. Ding, R. A. N. S. Ramos, H. Mohanram, K. Deepankumar, J. Gao, G. Tang and A. Miserez, *ACS Nano*, 2017, **11**, 4528-4541.
18 P. P. Neelakandan, Z. Pan, M. Hariharan, Y. Zheng, H. Weissman, B. Rybtchinski and F. D. Lewis, *J. Am. Chem. Soc.*, 2010, **132**, 15808-15813.
19 D. Ke, C. Zhan, A. D. Q. Li and J. Yao, *Angew. Chem. Int. Ed.*, 2011, **50**, 3715-3719.
20 T. Naota and H. Koori, *J. Am. Chem. Soc.*, 2005, **127**, 9324-9325.
21 K. Isozaki, H. Takaya and T. Naota, *Angew. Chem, Int. Ed.*, 2007, **46**, 2855-2857.
22 Y. Wang, C. Zhan, H. Fu, X. Li, X. Sheng, Y. Zhao, D. Xiao, Y. Ma, J. S. Ma and J. Yao, *Langmuir*, 2008, **24**, 7635-7638.
23 X. Yu, Q. Liu, J. Wu, M. Zhang, X. Cao, S. Zhang, Q. Wang, L. Chen and T. Yi, *Chem. Eur. J.*, 2010, **16**, 9099-9106.
24 R. M. Uda, E. Hiraishi, R. Ohnishi, Y. Nakahara and K. Kimura, *Langmuir*, 2010, **26**, 5444-5450.
25 X. Zhou, Y. Duan, S. Yan, Z. Liu, C. Zhang, L. Yao and G. Cui, *Chem. Commun.*, 2011, **47**, 6876-6878.
26 S. Yagai, K. Ishiwatari, X. Lin, T. Karatsu, A. Kitamura and S. Uemura, *Chem. Eur. J.*, 2013, **19**, 6971-6975.
27 D. J. van Dijken, J. Chen, M. C. A. Stuart, L. Hou and B. L. Feringa, *J. Am. Chem. Soc.*, 2016, **138**, 660-669.
28 T. Ikegami, Y. Kageyama, K. Obara and S. Takeda, *Angew. Chem. Int. Ed.*, 2016, **55**, 8239-8243.
29 G. Ashkenasy, T. M. Hermans, S. Otto and A. F. Taylor, *Chem. Soc. Rev.*, 2017, **46**, 2543-2554.
30 B. A. Grzybowski, K. Fitzner, J. Paczesny and S. Granick, *Chem. Soc. Rev.*, 2017, **46**, 5647-5678.
31 B. Adelizzi, N. J. Van Zee, L. N. J. de Windt, A. R. A. Palmans and E. W. Meijer, *J. Am. Chem. Soc.*, 2019, **141**, 6110-6121.
32 M. M. Safont-Sempere, G. Fernández and F. Würthner, *Chem. Rev.*, 2011, **111**, 5784-5814.
33 R. Eelkema, M. M. Pollard, J. Vicario, N. Katsonis, B. S. Ramon, C. W. M. Bastiaansen, D. J. Broer and B. L. Feringa, *Nature*, 2006, **440**, 163.
34 Z.-g. Zheng, Y. Li, H. K. Bisoyi, L. Wang, T. J. Bunning and Q. Li, *Nature*, 2016, **531**, 352-357.
35 K.-T. Wong and D. M. Bassani, *NPG Asia Materials*, 2014, **6**, e116.
36 S. Casalini, C. A. Bortolotti, F. Leonardi, and F. Biscarini, *Chem. Soc. Rev.*, 2017, **46**, 40-71.
37 X. Zhang, S. Rehm, M. M. Safont-Sempere and F. Würthner, *Nat. Chem.*, 2009, **1**, 623-629.
38 X. Zhang, Z. Chen and F. Würthner, *J. Am. Chem. Soc.*, 2007, **129**, 4886-4887.
39 C.-H. Hsu, X.-H. Dong, Z. Lin, B. Ni, P. Lu, Z. Jiang, D. Tian, A.-C. Shi, E. L. Thomas and S. Z. D. Cheng, *ACS Nano*, 2016, **10**, 919-929.
40 G. Fan, Y.-X. Lin, L. Yang, F.-P. Gao, Y.-X. Zhao, Z.-Y. Qiao, Q. Zhao, Y.-S. Fan, Z. Chen and H. Wang, *Chem. Commun.*, 2015, **51**, 12447-12450.
41 D. Görl, B. Soberats, S. Herbst, V. Stepanenko and F. Würthner, Chem. Sci. 2016, **7**, 6786-6790.
42 C. Weber, R. Hoogenboom and U. S. Schubert, *Prog. Polym. Sci.*, 2012, **37**, 686-714.
43 S. V. Aathimanikandan, E. N. Savariar and S. Thayumanavan, J. Am. Chem. Soc. 2005, **127**, 14922–14929.
44 E. Lee, Y.-H. Jeong, J.-K. Kim and M. Lee, *Macromolecules*, 2007, **40**, 8355-8360.
45 D. W. Chang and L. Dai, *J. Mater. Chem.*, 2007, **17**, 364-371.
46 J.-K. Kim, E. Lee, Y.-b. Lim and M. Lee, *Angew. Chem. Int. Ed.*, 2008, **47**, 4662-4666.
47 H. Hayashi, K. Ohkubo, S. Karasawa and N. Koga, *Langmuir*, 2011, **27**, 12709-12719.
48 L. Li, Y. Che, D. E. Gross, H. Huang, J. S. Moore and L. Zang, *ACS Macro Lett.*, 2012, **1**, 1335-1338.
49 P. Wei, T. R. Cook, X. Yan, F. Huang and P. J. Stang, *J. Am. Chem. Soc.*, 2014, **136**, 15497-15500.
50 S. Kashyap and M. Jayakannan, *J. Mater. Chem. B*, 2014, **2**, 4142-4152.
51 K. R. Raghupathi, U. Sridhar, K. Byrne, K. Raghupathi and S. Thayumanavan, *J. Am. Chem. Soc.*, 2015, **137**, 5308– 5311.
52 X. Yao, X. Wang, T. Jiang, X. Ma and H. Tian, *Langmuir*, 2015, **31**, 13647-13654.

53 J. Cui, J. E. Kwon, H.-J. Kim, D. R. Whang and S. Y. Park, *ACS Appl. Mater. Interfaces*, 2017, **9**, 2883-2890.
54 D. Kungwatchakun and M. Irie, *Macromol. Rapid Commun.*, 1988, **9**, 243-246.
55 T. Hirose, M. Irie and K. Matsuda, *Adv. Mater.*, 2008, **20**, 2137-2141.
56 T. Ogoshi, R. Shiga and T. Yamagishi, *J. Am. Chem. Soc.*, 2012, **134**, 4577-4580.
57 K. Higashiguchi, G. Taira, J.-i. Kitai, T. Hirose and K. Matsuda, *J. Am. Chem. Soc.*, 2015, **137**, 2722−2729.
58 H. Yotsuji, K. Higashiguchi, R. Sato, Y. Shigeta and K. Matsuda, *Chem. Eur. J.*, 2017, **23**, 15059-15066.
59 K. Higashiguchi, H. Yotsuji and K. Matsuda, *Chem. Lett.*, 2017, **46**, 1564-1566.
60 A. Sakaguchi, K. Higashiguchi and K. Matsuda, *Chem. Commun.*, 2018, **54**, 4298-4301.
61 A. Sakaguchi, K. Higashiguchi and K. Matsuda, *ChemPhotoChem*, 2017, **1**, 488-492.
62 A. Sakaguchi, K. Higashiguchi, H. Yotsuji and K. Matsuda, *J. Phys. Chem. B*, 2017, **121**, 4265-4272.

**Table of Contents graphic and text**

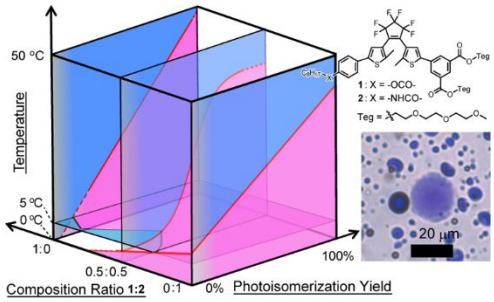


Supramolecular assembly composed of two-component mixture of amphiphilic diarylethenes showed separation into a blue sphere and a red-purple sparse structure by local LCST transition in the region of high fraction of the closed-ring isomer.